

Review

# Scope and Limitations of Modelling, Simulation, and Optimisation of a Spiral Wound Reverse Osmosis Process-Based Water Desalination

Alanood A. Alsarayreh <sup>1</sup>, Mudhar A. Al-Obaidi <sup>2</sup> , Raj Patel <sup>1</sup> and Iqbal M. Mujtaba <sup>1,\*</sup> 

<sup>1</sup> Department of Chemical of Engineering, Faculty of Engineering and Informatics, The University of Bradford, Bradford BD7 1DP, UK; A.A.M.Alsarayreh@bradford.ac.uk (A.A.A.); r.patel@bradford.ac.uk (R.P.)

<sup>2</sup> Middle Technical University, Technical Institute of Baquba, Baquba 00964, Iraq; dr.mudhar.alaubedy@mtu.edu.iq

\* Correspondence: I.M.Mujtaba@bradford.ac.uk; Tel.: +44-012-7423-3645

Received: 30 March 2020; Accepted: 26 April 2020; Published: 12 May 2020



**Abstract:** The reverse osmosis (RO) process is one of the best desalination methods, using membranes to reject several impurities from seawater and brackish water. To systematically perceive the transport phenomena of solvent and solutes via the membrane texture, several mathematical models have been developed. To date, a large number of simulation and optimisation studies have been achieved to gauge the influence of control variables on the performance indexes, to adjust the key variables at optimum values, and to realise the optimum production indexes. This paper delivers an intensive review of the successful models of the RO process and both simulation and optimisation studies carried out on the basis of the models developed. In general, this paper investigates the scope and limitations of the RO process, as well as proving the maturity of the associated perspective methodologies.

**Keywords:** water desalination; reverse osmosis process; spiral wound (SW) module; modelling; simulation; optimization

## 1. Introduction

The 21st century has been termed as the “century of water shortage”, and its first and second decades have been called “water crisis decades” [1]. This is associated with a progressive increase of population growth and elevated levels of fresh water demand. According to some reports issued by the World Health Organization (WHO), it is predicted that the half of the population in the world will live in water-stressed regions by 2025. This means that about 2.1 billion people in the world will find it difficult to have access to safe drinking water [2]. Another report from the United Nations World Water Assessment Program confirmed that one-fifth of the world’s inhabitants are facing shortage of fresh water resources. In the meantime, several Middle Eastern, South East Asian, and North African countries are struggling from water shortage and have been classified as water-stressed areas due to a lack of rainwater and water resource pollution [3]. Accordingly, this scarcity is expected to affect up to 40% of the world’s population by 2030. The improvement of seawater and brackish water desalination technologies is thus a pressing need. In essence, desalination is a water treatment process that produces fresh water from high salinity water by removing the dissolved salts and other contaminants. Therefore, desalination is widely deployed to enhance the quality of high-salinity seawater and low-salinity brackish water. Specifically, the desalination process involves the filtration of feed saline water that produces low-salinity water and brine (very concentrated water) [4].

Indeed, there was a clear incline and increased application of seawater and brackish water desalination in the world, especially in the Gulf region, as the main technology for supplying fresh water. The Middle East has thus prevailed in the global desalination market over the last decades

(Figure 1). Many of the world's desalination plants are situated in Gulf Cooperation Council (GCC) countries that comprise Qatar, Saudi Arabia, United Arab Emirates (UAE), Kuwait, Oman, and Bahrain. On the basis of the statistical data presented by the International Energy Agency (IEA), about 58% of total desalination capacity in the world lies in the Middle East and North Africa, as shown in Figure 1 [5]. Specifically, reverse osmosis (RO) desalination projects have been remarkably increased and expanded, especially between 2014 and 2016. For instance, the RO desalination plant of Ras Al-Khair located in Saudi Arabia associated with fresh water capacity of 1,025,000 m<sup>3</sup>/day in 2014 [6]. Undoubtedly, the progressive increased line of water shortage would contribute to an increase in the global desalination market by 2025, as expected by the United Nations Department of Economic and Social Affairs (UNDESA). Historically, the first large scale desalination units were installed in the Middle East in Kuwait in the 1950s. The world's biggest RO plant, at a capacity of 274,000 m<sup>3</sup>/day, was constructed in southern Arizona [7].

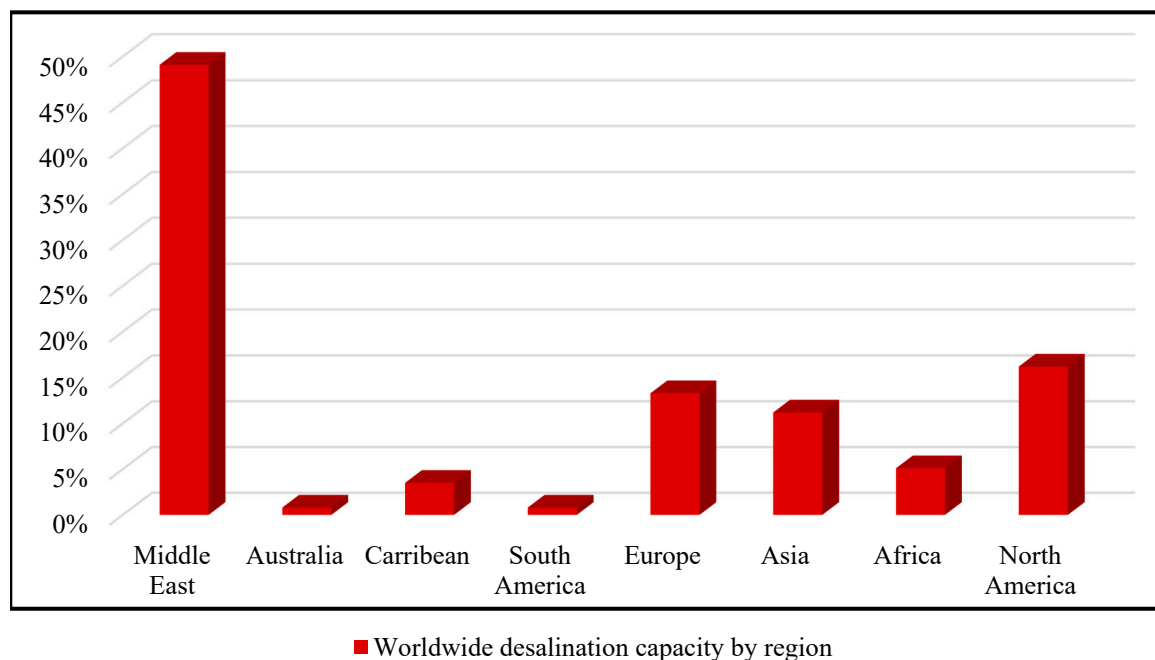


**Figure 1.** The desalination capacity worldwide, shown on the basis of region.

According to the level of salinity, water can be classified into three types [8];

- Seawater with concentration of 35,000 ppm of total dissolved solids or more.
- Brackish water with concentration between 1000–15,000 ppm of TDS (Total Dissolved Solids).
- Fresh water with concentration below 500 ppm of TDS.

To the best of the authors' knowledge, a critical evaluation of spiral wound (SW) RO process-based seawater and brackish water desalination including its modelling, simulation, and optimisation aspects has not been presented in the open literature. Therefore, this paper attempts to introduce a comprehensive review to overcome this challenge and to elucidate several suggestions to enable optimal operation of the RO process.

## 2. Reverse Osmosis Process

The use of RO desalination process has increased significantly in recent years and comprises about 80% of the total desalination plants worldwide. The RO process was deliberated as the most promising technology for seawater and brackish desalination [9]. Figure 2 shows the domination of RO process at a capacity of 44% of the total worldwide fresh water production. The other technologies

of multi-stage flash (MSF), electrodialysis (ED), vacuum compression (VC), multiple effect distillation (MED), and other distillation processes have capacities of 40%, 6%, 5%, 3%, and 2%, respectively.

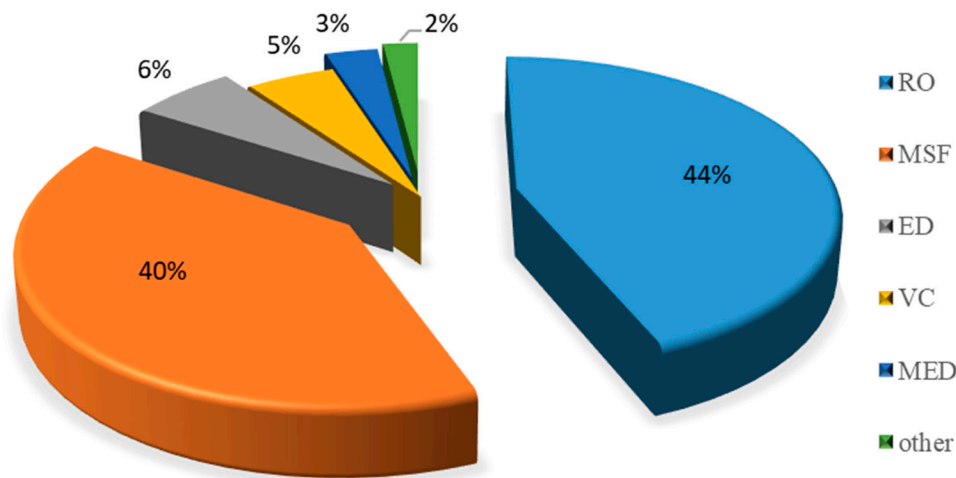


**Figure 2.** The distribution of desalination capacity for different processes (adapted from Greenlee et al. 2009) [5].

The RO process falls under the membrane process category, which is founded on the theory of solvent and solute migration via a semi-permeable medium. This theory constitutes the fact of natural osmosis, which denotes the moving of water from a lower salinity medium to a higher salinity medium. High pressure is required on the higher concentration side to move the water from the higher concentration medium to the lower concentration medium along a partially permeable membrane. Specifically, the RO process is operated by pressurising the saline feed water into a closed vessel using high-pressure pumps beyond osmotic pressure, which is proportionate to the solute's concentration in the pumped water. Therefore, the water passes through the membrane towards the low concentration side, producing fresh water at the permeate channel and brine (high-concentration) leaving the unit. It is noteworthy that the feed water becomes gradually concentrated along the membrane channel as a result of the permeated water, becoming progressively more concentrated. Moreover, the quality of the feed water and operating conditions are the most highlighted indicators related to the performance of a RO system. Ultimately, the two characteristics of water quantity and quality need to be maximised for the most efficient and economical desalination technology. These two features are adversely sensitive to fouling, compaction, and hydrolysis. Practically, RO processes require high feed pressure to tackle the decreasing in water productivity and to preserve a fixed production rate. However, this would definitely lead to a high-cost of water production. Moreover, the forecast of long-term performance is crucial for an efficacious operation of RO system, which can be achieved via process modelling [10].

The RO process has several merits including its reliability and maturity at low investment costs at low capacities coupled with low maintenance cost. As well as this, deteriorated and aging or excessive fouled RO membrane modules can be easily replaced, together with the flexibility of adding new modules to suit any required water quantity and quality with short implementation periods [11]. Moreover, RO processes operate at ambient temperatures unlike thermal desalination processes [4]. In addition, RO processes have a high quality of coinciding elimination of both inorganic and organic pollutants, low ejection in the brine stream, and lower energy requirements than equivalent thermal processes. The RO process accounted more than 60% of the market share in 2017 [12]. Therefore, it is not surprising to notice different sizes of RO plants, ranging from small scale, to medium scale, to large scale. In essence, any practical RO plant has to have essential components, including high-pressure pumps, membrane modules, and energy recovery devices [13,14]. The single biggest disadvantage of the RO process is the limited retardation of water recovery. For instance, seawater can be desalinated as fresh water at around 35%–40%, compared to 90% of water recovery for brackish water [13,14].

The low water recovery of the RO process is attributed to its propensity of fouling. It is well known that the membrane fouling of the RO process is specifically related to the type of feed water and requires careful monitoring and control of the operating conditions. The largest energy input in a RO plant is the electric power needed to operate the high-pressure pumps for pressurising the high concentration feed. However, the specific energy consumption of the RO process is lower compared to other thermal desalination processes such as MSF or MED. [15] concluded that the RO process consumes half the energy needed for the thermal desalination process. With the acknowledgment of indirect comparison, the electrical energy consumption of a RO process is 3 to 4 kWh/m<sup>3</sup> compared to 5.5 to 16 kWh/m<sup>3</sup> for MSF and MED processes [6]. Interestingly, the energy consumption of the RO process can be condensed by 30% as a result of adding an energy recovery device to the brine stream. In this regard, seawater and brackish water require a range of pressures of 55 to 68 atm and 17 to 27 atm, respectively [13,14].

Several types of RO membrane modules have been designed by membrane producers to costume several determinations such as the SW module, which is one of the best economic modules of the RO process compared to other modules of tubular, hollow-fibre, and plate and frame. In addition, the membranes are designed specifically as high-flux and high-retention membranes, besides fouling resistant membranes (appropriate for high-salinity seawater causes extreme fouling). Finally, SW membrane (the aim of this research) has affirmed its consistency in seawater and brackish water desalination. The next section discusses the most promising characteristics of the SW module and its limitations.

### *Spiral Wound Module*

The spiral wound (SW) module is made from rolled membrane sheets around a collected central perforated tube of fresh water and is separated by high-porous spacers to enabling water transport to the central tube. Therefore, the membrane sheets are kept apart by using the spacers that enhance mixing and turbulence inside the module, and consequently increase mass transport along the membrane surface and reduce the concentration polarisation [16].

Figure 3 depicts a schematic diagram of a SW module. This module has been considered as one of the most effective modules from all the different ones utilised in RO processes. This is due to its high productivity per unit volume as a result of its large ratio of surface to volume. Additionally, it is characterised by its simple fabrication technology, ease of operation and cleaning, and compact size [17,18]. In addition, it has characterised by its low propensity of fouling besides its ease of operation. This is probably the reason why SW modules are used for water desalination in remote areas [19]. Due to the advantage of these techno-economic factors, SW RO process modules have the largest market share, with a noticeable growth of its use in different filtration fields such as wastewater treatment and beverage production besides seawater and brackish water desalination [20].

Generally, understanding the transport phenomena of water and solute movement via the membrane structure is vital in order to have an efficient RO treatment process. Therefore, a precise model is required to evaluate the performance of RO membrane via correlating the main operating conditions and the performance indicators. In this regard, the process simulation and optimisation can be carried out on the basis of the process modelling. The merits of RO process modelling, simulation, and optimisation are as follows:

1. The importance of RO process modelling
  - A paramount tool to analysis and design the RO system.
  - To forecast the long-term performance using the dynamic modelling version. Thus, the decision-makers can forecast when to change the membrane elements.
  - To predict the performance of different designs of RO systems.
  - To be combined with the cost model to assess the water production cost of RO systems.
  - To carry out extensive simulation and optimisation studies to improve the process performance.
2. The importance of simulation

- To conceive the power of operating conditions on the performance indicators of solute removal and water recovery.
- To analyse the effect of operating conditions on the total energy consumption.
- A simulator tool can be used for process training and examining without the risk of damaging the equipment.
- To obtain suitable operating conditions to maintain the highest performance.
- To aid the process design and select the best membrane area to achieve highest recovery.
- To carry out the process optimisation in order to progress the process operation and selecting the optimal operating conditions and process control.

### 3. The importance of optimisation

- To forecast the appropriate values of the control variables of the RO process that would attain the highest water recovery and lowest fresh water concentration.
- To obtain the optimal configuration of the multistage RO process by considering a set of several constraints communicated to the unit's equations or including inequalities to yield the favourite optimum responses.
- To minimise the total fresh water production cost whilst maintaining maximum quantity and quality of product water.
- To improve the design, operation, and assembly of multistage RO process at different periods of its life cycle.
- To reduce the total energy consumption of the RO process by delivering a high-performance ratio and stable operation.
- To mitigate the fouling propensity of the RO process by selecting the optimum control variables and process design.

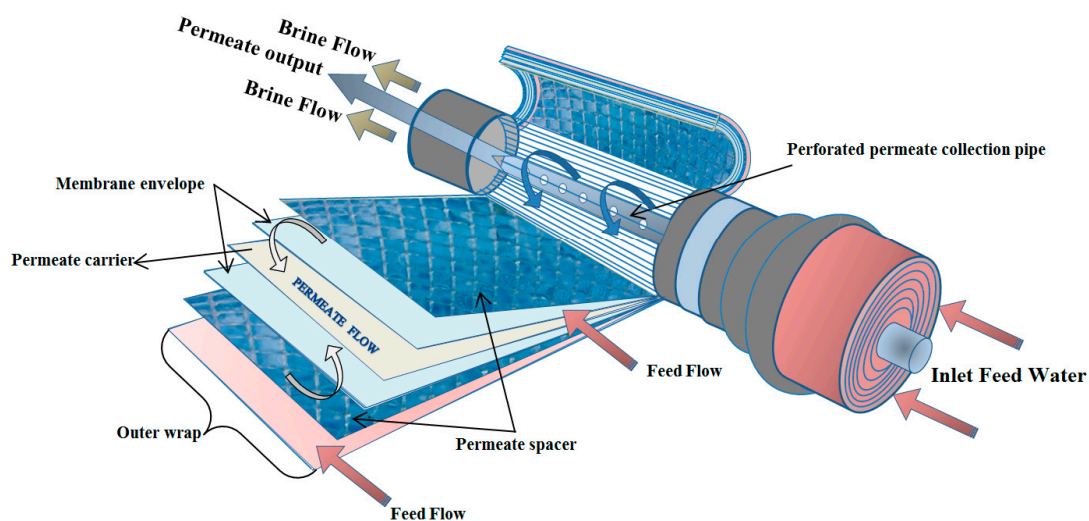


**Figure 3.** Schematic diagram of a spiral wound (SW) membrane element (Adapted from Additive Manufacturing, 2020) [21].

An overview of the modelling, simulation, and optimisation of the SW RO process is thoroughly outlined in the following sections.

### 3. Overview of Modelling of a Spiral Wound RO Module

Modelling of industrial processes is essential because it recognises the process mechanism and realises the intercorrelation between the process variables and its responses. This in turn enables the assessment of the influence of each control variable, which aids to allocating the

objective functions through process simulation and optimisation. For instance, the modelling of the RO process helps to understand the contribution of all control variables that control the process performance without resorting to carrying out extensive, expensive, and complicated experiments. Therefore, the relationship between the relevant RO process indicators, such as water recovery ratio, energy consumption, and solute rejection, with the control variables of feed flow rate, pressure, temperature, and designing variables of the membrane module dimensions can be outlined via simulation. Furthermore, the process variables can be optimised without applying any changes in the real plant via optimisation. Therefore, it is not surprising to find many serious attempts of modelling the SW RO process in the open literature. In this aspect, Oh et al. [22] reported that the obtainability of a consistent RO model is of pronounced status for process design and operation. Therefore, generating rigorous models that could efficiently forecast the process mechanism was the main aim. However, several mathematical models were developed on the basis of strict assumptions or relaxing reliable assumptions that entailed with a noticeable simplicity or difficulty of process modelling. Specifically, the complex models of the RO process have included membrane fouling, concentration polarisation, pressure drop, and membrane aging. On the other hand, the simple models have relaxed the membrane fouling and ignored the concentration polarisation. In addition, several models have been proposed involving fixed mass transfer and permeate pressure at the permeate channel.

The earliest mathematical models (~1965) were developed to specify the transport phenomena of the RO process, including both water and solute permeation via the membrane structure. This was specifically carried out by the investigation of two parental theories of the solution–diffusion model (homogeneous membrane model) and the irreversible thermodynamic model [16,20,23,24]. This was followed by the development of several models to represent different complexity of transport phenomena for different RO process modules and feed type (seawater, brackish water, wastewater), which were based on the original basic models.

The next section presents in detail the state-of-the-art of modelling of the SW RO desalination process.

### 3.1. Model of Lonsdale et al.

Lonsdale et al. [25] developed the basic solution–diffusion model (homogeneous or non-porous membrane model). They assumed that both solvent and solute are separately diffused from the high-concentration and pressure side to the low-concentration and pressure side, at different rates of diffusion, via the membrane texture due to the pressure and concentration gradient along the feed and permeate channels. In this regard, the total water flux ( $J_w$ ) (m/s) and solute flux ( $J_s$ ) (kmol/m<sup>2</sup> s) are determined on the basis of their diffusion mechanism, which is related to their solubility and solute mobility:

$$J_w = A_w (\Delta p - \Delta \pi) = A_w \left( (P_r - P_p) - RT (C_r - C_p) \right) \quad (1)$$

$$J_s = B_s (C_r - C_p) \quad (2)$$

Water permeability coefficients (m/s Pa) are expressed as  $A_w$ . Moreover,  $\Delta p, \Delta \pi, P_r, P_p, R, T, C_p, C_r$ , and  $B_s$  express the hydraulic pressure difference (Pa), osmotic pressure difference (Pa), the brine pressure (Pa), the permeate pressure (atm), gas law constant (8.314 J/mol K), temperature (K), permeate concentration (kmol/m<sup>3</sup>), retentate concentration (kmol/m<sup>3</sup>), and salt permeability coefficient (m/s), respectively. It is worth noting that Lonsdale et al. [26] assumed that solute flux does not rely on the pressure difference (Equation (2)). Interestingly, realising of water and solute transport parameters is critical to predict the solvent and solute fluxes. However, ignoring both the pressure influence on the solute flux and the membrane characteristics are the main disadvantages of this model.

### 3.2. Model of Boudinar et al.

Boudinar et al. [26] established a mathematical model for a SW module considering the main parameters, which affect its performance based on the solution–diffusion model. The model considered

the fact that the pressure loss in the feed and permeate channels are controlled by feed and permeate friction parameters on the basis of the theory of Darcy for porous media. The features of the developed model are as follows:

### 3.2.1. Assumptions

- Validity of the solution–diffusion model to specify the solvent and solute transport mechanisms.
- Ignoring the variation of brine and permeate along axial and radial directions.
- Fixed fluid physical properties such as density and viscosity.
- The pressure change is neglected at the permeate collector tube.

### 3.2.2. Model Equations

The solvent and solute fluxes via the membrane are measured using Equations (1) and (2), respectively. However, the water and solute permeability constants are estimated as

$$A_w = K_{10} \times 10^{-5} \exp^{-1.701 \times 10^2 P_f} \quad (3)$$

$$B_s = 1.112 \times 10^{-6} \exp^{274.15 \times 10^{-2} T} \quad (4)$$

Water permeability coefficient at zero pressure (m/s Pa) is expressed as  $K_{1.0}$ , whereas  $P_f$  and  $T$  are the feed pressure (Pa) and temperature (K), respectively. Equation (5) expresses the correlation between water flux and solute flux to calculate the permeate concentration:

$$C_p = \frac{J_s}{J_w + J_s} = \frac{J_s}{J_w} = \frac{B_s (C_r - C_p)}{J_w} \quad (5)$$

The retentate concentration  $C_r$  (kmol/m<sup>3</sup>) is estimated by a material balance equation, as follows:

$$C_r = \frac{C_f Q_f - C_p Q_p}{Q_r} \quad (6)$$

The feed concentration is  $C_f$  (kmol/m<sup>3</sup>), and  $Q_f$ ,  $Q_p$ , and  $Q_r$  represent the feed flow rate (m<sup>3</sup>/s), product flow rate (m<sup>3</sup>/s), and retentate flow rate (m<sup>3</sup>/s), respectively. The mass transfer coefficient  $k$  (m/s) and solute concentration at the membrane wall  $C_w$  (kmol/m<sup>3</sup>) are

$$J_w = k \ln \left[ \frac{C_w - C_p}{C_r - C_p} \right] \quad (7)$$

The osmotic pressure at operating temperature  $\pi_{T_i}$  (Pa) is calculated on the basis of osmotic pressure at 25 °C ( $\pi_{T_{25}}$  (Pa)) as

$$\frac{\pi_{T_i}}{T_i} = \frac{\pi_{T_{25}}}{T_{25}} \quad (8)$$

$$\pi_{T_{25}} = 0.23745 + 6.4784 \times 10^{-4} C_b \quad (9)$$

The bulk concentration is  $C_b$  (kmol/m<sup>3</sup>). The physical properties of viscosity  $\mu$  (kg/m s) and diffusion coefficient  $D_s$  (m<sup>2</sup>/s) correlations are calculated using Equations (10) to (12).

$$\mu = 0.1 \mu_0 \exp^{-2.008 \times 10^{-2} T} \quad (10)$$

$$\mu_0 = 1.4757 \times 10^{-2} + 2.4817 \times 10^{-8} C_b + 9.3287 \times 10^{-14} C_b^2 \quad (11)$$

$$D_s = (0.72598 + 2.3087 \times 10^{-2} T + 2.7657 \times 10^{-4} T^2) \times 10^{-9} \quad (12)$$

### 3.3. Model of Avlonitis et al.

Avlonitis et al. [27–29] presented steady state distributed models instituted on the solution–diffusion model and the thin film theory to study the performance of SW modules.

#### 3.3.1. Assumptions

- The module is made up of a flat channel with fixed geometry.
- Variable fluid flow rate along the  $x$ -axis of feed channel and  $y$ -axis of permeate channel.
- Fixed fluid flow rate across the  $y$ -axis of feed side and  $x$ -axis of permeate side.
- Fixed mass transfer coefficient and physical properties.
- Fixed permeate concentration at the permeate channel.
- Fluid velocity specifies the friction parameters of the feed and permeate channels.

#### 3.3.2. Model Equations

The brine and the permeate friction parameters at different Reynolds numbers can be calculated using Equations (13) and (14), respectively.

$$K_{fr} = 0.309 R_{er}^{0.83} \quad (13)$$

$$K_{fp} = 46.2915 R_{ep}^{0.26} \quad (14)$$

The retentate and permeate friction parameters ( $m^2$ ) are represented as  $K_{fr}$  and  $K_{fp}$ , respectively, and  $R_{er}$  and  $R_{ep}$  (dimensionless) are the Reynolds number at retentate and permeate channels, respectively. The water permeability coefficient  $A_w$  depends on the operating temperature and applied pressure:

$$A_w = 2.955 \times 10^{-5} \exp\left(10.27 \frac{T - T_{293.15}}{T_{293.15}} - 0.0015 P_f\right) \quad (15)$$

The solute transport parameter is expressed as a function of the applied temperature, as depicted in Equation (16).  $T_{293.15}$  is the operating temperature at 20 °C.

$$B_s = 9.54 \times 10^{-7} \exp^{14.648 \frac{T - T_0}{T_0}} \quad (16)$$

The absolute temperature is  $T_0$  (K) at 20 °C.

### 3.4. Model of Abbas and Al-Bastaki

Abbas and Al-Bastaki [10] presented a complete model to expect the performance of an SW membrane module. Both turbulent and laminar flow regimes were considered in the model. However, the diffusivity is assumed constant.

#### Model Equations

Equations (17) and (18) are used to assess turbulent and laminar flow regimes Wilf and Klinko [30], respectively:

$$Sh = 0.04 R_e^{0.75} Sc^{0.33} \quad \text{for turbulent flow} \quad (17)$$

$$Sh = 1.86 (R_e Sc d_h / L)^{0.33} \quad \text{for laminar flow} \quad (18)$$

Sherwood number is expressed as  $Sh$  (dimensionless), whereas  $Sc$ ,  $L$ , and  $d_h$  are Schmidt number (dimensionless), membrane length (m), and hydraulic diameter of the flow channel (m), respectively. The water  $A''_w$  (m/s Pa) and solute  $B''_s$  (kg/m<sup>2</sup> s Pa) permeability constants were determined on the basis of the operating time  $t$  (day).

$$A''_w = \frac{168 + 0.68 t}{166.3 + t} \times 10^{-5} \quad (19)$$

$$B_s'' = 0.68 \times 10^{-5} \exp\left(\frac{79}{T+201.1}\right) \quad (20)$$

The water flux and mass transfer coefficient are the same as those used by Boudinar et al. [26].

### 3.5. Model of Marriott and Sørensen

Marriott and Sørensen [31] established a distributed dynamic model for an SW RO module by implementing mass balance, momentum, and energy equations, and by disregarding some mutual assumptions. This model describes the flow patterns inside the module and can be applied to any membrane separation. However, the variation of bulk concentration inside the feed channel due to solvent flux through the membrane was not entirely considered.

#### 3.5.1. Assumptions

- The flow behaviour in the module is not affected significantly by the bent channel.
- The channel curvature is negligible.
- The stagnant model describes the concentration polarisation.
- The friction parameter signifies the pressure drop along the feed channel.
- The pressure and temperature in feed channel are assumed constant.
- Fixed physical properties of the fluid.
- Steady state plug flow (no concentration variation in the perpendicular direction) inside the feed channel.

#### 3.5.2. Model Equations

Water (permeate) and solute (retentate) fluxes are represented as

$$J_w = A_w C_p (\Delta P - \Delta \pi) \quad (21)$$

$$J_s = B_s (C_f - C_p) \quad (22)$$

### 3.6. Model of Abbas and Al-Bastaki

Abbas and Al-Bastaki [32] proposed a semi-rigorous model to inspect the performance of a RO desalination plant designed in three tapered stages. The developed model is able to predict future plant performance.

#### Model Equations

The water and salt fluxes are calculated on the basis of Sourirajan [33] relations as follows:

$$Q_p = J_w A_m = A_m \frac{\Delta p - \Delta \pi}{(1.142 \times 10^{-10} R_p)} \quad (23)$$

$$J_s = \frac{C_w - C_p}{R_r} \quad (24)$$

Total production permeate capacity is represented as  $Q_p$  ( $\text{m}^3/\text{s}$ ), and  $A_m$ ,  $R_p$ , and  $R_r$  are the effective membrane area ( $\text{m}^2$ ); permeate membrane resistance, which is equal to  $(\frac{1}{B_s})$  ( $\text{s}/\text{m}$ ); and retentate membrane resistance ( $\text{s}/\text{m}$ ), respectively. The bulk concentration  $C_b$  ( $\text{kmol}/\text{m}^3$ ) and bulk flow rate  $Q_b$  ( $\text{m}^3/\text{s}$ ) can be calculated on the basis of their relative values on the feed and retentate sides:

$$C_b = \frac{C_f + C_r}{2} \quad (25)$$

$$Q_b = \frac{Q_f - Q_r}{2} \quad (26)$$

Water recovery (dimensionless) and solute rejection (dimensionless) are used to evaluate the performance of RO process as follows:

$$WR = \frac{Q_p}{Q_f} \times 100 \quad (27)$$

$$SR = \frac{C_f - C_p}{C_f} \times 100 \quad (28)$$

### 3.7. Model of Geraldles et al.

Geraldles et al. [34] improved a steady state distributed model for a SW seawater RO process considering the mass and momentum transport inside the membrane modules. The model is substantially settled on the basis of the solution–diffusion and ignores the diffusion flow in the feed channel and the pressure variation along the permeate channel.

#### 3.7.1. Assumptions

- Plug flow occurs in the feed channel.
- Concentration polarisation is considered on the basis of the film theory.
- The decrease of pressure inside the permeate channel is neglected.
- Physical properties of seawater are correlated on the basis of temperature and concentration.

#### 3.7.2. Model Equations

Water and solute fluxes are expressed in Equations (29) and (30)

$$J_w = A_w [P_f - \pi_m + \pi_p] \quad (29)$$

$$J_s = B_s (C_r - C_p) \quad (30)$$

The osmotic pressures of the feed water at high-concentration and low-concentration channels are denoted as  $\pi_m$  and  $\pi_p$  (Pa), respectively. Moreover,  $C_p$  is the permeate concentration, which is calculated via Equation (31):

$$C_p = \frac{J_s}{J_w} \quad (31)$$

The mass transfer coefficient  $k$  (m/s) is derived from the following correlation:

$$Sh = 0.065 Re^{0.875} Sc^{0.25} = k 6.23 Re^{-0.3} \quad (32)$$

### 3.8. Model of Avlonitis et al.

Avlonitis et al. [29] developed an extensive mathematical model to calculate the performance of any type of RO membrane modules. Their model considered both axial and tangential dimensions of RO membrane to determine the quality of the produced water.

#### Model Equations

Equations (33), (34), and (35) are used to estimate the brine friction parameter, water permeability coefficient, and salt permeability coefficient, respectively.

$$k_{fr} = 309 \times Re_f^{0.83} \quad (33)$$

$$A_w = K_{1m} \exp^{8.6464 \left( \frac{T-T_{20}}{T_{20}} \right) - 0.0028 P_f} \quad (34)$$

$$B_s = K_{2m} \exp^{14.648 \left( \frac{T-T_0}{T_0} \right)} \quad (35)$$

Two symbols of  $K_{1m}$  and  $K_{2m}$  are constants that depend on membrane type.

### 3.9. Model of Majali et al.

Majali et al. [35] developed two models for two pilot-scale RO plants to analyse their performances. Firstly, a semi-empirical simple model was developed for a RO Sharjah plant used to desalinate brackish water. This model predicted flow rate, concentration, and pressure profiles but ignored the membrane area. Secondly, a permeability model was proposed to predict the performance of an RO plant in Qatar that desalinates high salinity seawater. Interestingly, the model predicts the membrane area. The model's assumptions are as follows:

#### 3.9.1. Assumptions

- Steady state and isothermal operation.
- Fixed salt rejection and recovery for each membrane module for the semi-empirical model.
- Fixed water and salt transfer parameters along the membrane for the permeability model.
- Atmospheric pressure inside the permeate channel.

#### 3.9.2. Model Equations of a Semi-Empirical Simple Model of Majali et al.

Equations (36) and (37) show the mass and salt balances on the SW membrane module for both semi-empirical and permeability models:

$$Q_f = Q_r + Q_p \quad (36)$$

$$Q_f C_f = Q_r C_r + Q_p C_p \quad (37)$$

The product recovery and salt rejection represent the most necessary performance indicators,

$$Q_p = WR Q_f \quad (38)$$

$$C_p = C_f (1 - SR) \quad (39)$$

The pressure drop and the osmotic pressure are given in Equations (40) and (41), respectively.

$$\Delta p = 0.5 (P_f + P_r) - P_p \quad (40)$$

$$\Delta \pi = RT \frac{\rho}{MW} \left( \frac{C_f Q_f + C_r Q_r}{Q_{f+Q_r}} - C_p \right) \quad (41)$$

The water density is represented as  $\rho$  (kg/m<sup>3</sup>), and  $MW$  is the salt molecular weight (kg/kmol).

#### 3.9.3. Model Equations of an Advanced Model of Majali et al.

The permeability model was developed on the basis of the mechanical–statistical model that was essentially established by Mason and Lonsdale [36]. This model includes the mass and salt balance equations of Equations (42) and (43), and the following relations give the water and salt fluxes:

$$Q_p = (\Delta P - \Delta \pi) A_w A_m \quad (42)$$

$$C_p Q_p \rho = \left( \frac{C_f Q_f + C_r Q_r}{Q_{f+Q_r}} - C_p \right) B_s A_m \quad (43)$$

### 3.10. Model of Oh et al.

Oh et al. [25] improved a simple mathematical model on the basis of the solution–diffusion principles and by considering the impact of multiple fouling of the SW seawater RO system.

#### 3.10.1. Assumptions

- Constant water flux and mass transfer coefficient after varying the inlet feed flow rate.
- Constant permeate pressure at the permeate channel.
- The osmotic pressure is proportionated to the solute concentration.

#### 3.10.2. Model Equations

Water permeation through the membrane structure is formulated to consider the pressure loss along the membrane feed channel:

$$J_w = A_w (P_f - P_{loss}) \quad (44)$$

The pressure loss is represented as  $P_{loss}$  (Pa). However, the solute flux equation of Lonsdale et al. (1965) is used. The osmotic pressure is expressed as

$$\Delta\pi = (C_r - C_p) R T \quad (45)$$

### 3.11. Model of Lee et al.

A complete dynamic model was developed by Lee et al. [37] on the basis of the work of Lee and Lueptow, Marriott and Sørensen, and Oh et al. [25,38,39]. Lee et al. [37] investigated the dynamic features, process design, and operation of the Jeddah large-scaled RO desalination plant with a production capacity of 56,800 m<sup>3</sup>/day that is located in the Kingdom of Saudi Arabia. The assumptions were the same as the previous models, except that the RO process was considered as a dynamic operation.

#### Model Equations

On the basis of steady-state membrane transport, the solvent flux equation is depicted as

$$J_w = A_w (P_f - P_{loss}) = A_w [P_f - (\Delta\pi + P_{drop})] \quad (46)$$

The pressure drop along the  $x$ -axis of feed side is represented as  $P_{drop}$  (atm). The solute transport parameter is obtained from

$$B_s = B_{s0} \exp \frac{\beta_1(T-273)}{273} \quad (47)$$

The intrinsic and fixed solute transport parameters are  $B_{s0}$  and  $\beta_1$  (dimensionless), respectively. The concentration polarisation  $\phi$  (dimensionless) is given by Equation (48).

$$\phi = \frac{C_w - C_p}{C_r - C_p} = \exp \frac{B_s}{k} \quad (48)$$

The mass transfer coefficient  $k$  (m/s) for the bulk diffusion of the solute is expressed as

$$k = 0.551 \left( \frac{u_f d_h}{\nu} \right)^{0.4} \left( \frac{\nu}{D_s} \right)^{0.17} \left( \frac{C_r}{\rho} \right)^{-0.77} \left( \frac{D_s}{d_h} \right) \quad (49)$$

The feed solution velocity on the bulk high-concentration side is expressed as  $u_f$  (m/s), and  $\nu$  denotes the kinematic viscosity (cm<sup>2</sup>/s). The dynamic equation of retentate concentration ( $C_r$ ) along the length membrane ( $x$ \_ dimension

(m)) is derived as

$$\frac{\partial C_r}{\partial t} = -\frac{\partial}{\partial x} \left( C_r u_f - D_s \frac{\partial C_r}{\partial x} \right) - \frac{1}{d_h} J_s \quad (50)$$

### 3.12. Model of Kaghazchi et al.

Kaghazchi et al. [20] utilised a steady state model grounded on the theory of the solution–diffusion model for the SW membrane module to examine the performance of two industrial seawater RO plants. The equations of Abbas and Al-Bastaki [32] have been used to forecast the water and salt fluxes, water recovery, and salt rejection. Interestingly, Kaghazchi et al. [20] considered the variation of operating conditions along the feed channel axis.

### 3.13. Model of Ruiz-Saavedra et al.

A simple model was invented by Ruiz-Saavedra et al. [39] for a SW brackish water RO plant located in Spain. The model included the fundamental operational data of the plant, such as the chemical composition, pH, silt density index (SDI; is expressed as the flux decline calculated by differentiating the initial flux to the flux after a constant time), and temperature. It is able to calculate the product concentration and quantity, taking into account the manufacturer's membrane design guidelines. The model assumptions considered were similar to those that have been presented in the previously developed models.

#### Model Equations

The water flow rate  $Q_{pi}$  ( $\text{m}^3/\text{s}$ ) through a membrane element  $i$  in a series of membrane elements stuffed in a pressure vessel is calculated as

$$Q_{pi} = A_{wi} (\Delta P_i - \Delta \pi_i) A_{mi} \quad (51)$$

Water permeability constant of the membrane element  $i$  is  $A_{wi}$  ( $\text{m}/\text{Pa s}$ ), and  $\Delta P_i$ ,  $\Delta \pi_i$ , and  $A_{mi}$  are the pressure drop across the membrane element  $i$  (Pa), the differential osmotic pressure along the membrane element  $i$  (Pa), and the membrane surface area ( $\text{m}^2$ ) of the membrane element  $i$ , respectively. The salt flux  $J_{si}$  ( $\text{kmol}/\text{m}^2 \text{ s}$ ) via the membrane element  $i$  is formulated as

$$J_{si} = B_{si} \Delta C_i A_{mi} \quad (52)$$

The salt permeability constant of the membrane element  $i$  ( $\text{m}/\text{s}$ ) and the differential solute concentration along the membrane element  $i$  ( $\text{kmol}/\text{m}^3$ ) are expressed as  $B_{si}$  and  $\Delta C_i$ , respectively. The osmotic pressure of the average concentration of the RO element  $i$   $\pi_{fri}$  (Pa) is expressed as

$$\pi_{fri} = \pi_{fi} WR_i CP_i \quad (53)$$

The osmotic pressure of the feed concentration of membrane element  $i$   $\pi_{fi}$  (Pa). Moreover,  $WR_i$  and  $CP_i$  are the water recovery of membrane element  $i$  and the concentration polarisation of  $i$ , respectively.

### 3.14. Model of Kotb et al.

Kotb et al. [40] developed a simple model by considering several layouts for two modules of RO systems to study concentration polarisation. The model developed was based on the same set of assumptions as those made by Boudinar et al. [26], ignoring the module pressure drop.

## Model Equations

The volumetric brine flow rate and concentration are calculated on the basis of Equations (7) and (36), respectively.

The water flux via a membrane is estimated on the basis of Wiley et al. (1985), whereas the solute flux is calculated by Equation (30).

$$J_w = A_w P_{eff} \quad (54)$$

The residual transmembrane pressure is represented as  $P_{eff}$  (Pa).

$$P_{eff} = (P_f - P_p - \Delta P - \frac{\Delta p_f}{2}) - (\pi_w - \pi_p) \quad (55)$$

The pressure drop in membrane module channel  $\Delta p_f$  (Pa) consists of pressure losses in the inlet and outlet module manifolds ( $\Delta p_{in}$  and  $\Delta p_{out}$ ) (Pa). The osmotic pressure at the membrane wall and permeate channel are  $\pi_w$  and  $\pi_p$  (Pa), respectively. The correlation of Maskan et al. [41] is deployed to guess the mass transfer coefficient

$$k = 1.62 \left( \frac{Re Sc d_{ch}}{L} \right)^{0.33} \frac{D_s}{d_{ch}} \quad Re \leq 2100 \quad (56)$$

$$k = 0.023 Re^{0.875} Sc^{0.25} \frac{D_s}{d_{ch}} \quad Re > 2100 \quad (57)$$

The membrane channel diameter is  $d_{ch}$  (m).

### 3.15. Model of Dimitriou et al.

Dimitriou et al. [42] established a model on the basis of the solution–diffusion and film theory for an SW RO membrane module. Several parameters along the  $x$ -axis of feed channel are explored, including the solute and solvent fluxes, concentration at the retentate and permeate sides, and pressure drop in the membrane element under different pressure and flow rate operation. Therefore, variable values of the solute concentration, pressure, and fluid velocity at feed and permeate sides are evaluated at each point along the  $x$ -direction.

#### 3.15.1. Assumptions Made

- The physical properties of fluid are a function of the salinity and temperature.
- Flat feed and permeate channel profiles. Specifically, the channel thickness is apparently lower than the radius of the module.
- Plug flow in both feed and permeate channels.

#### 3.15.2. Model Equations

The total water flux  $J_{total}$  ( $\text{kg}/\text{m}^2 \text{ s}$ ) via the membrane structure is simultaneously represented as the summation of water  $J_w$  and solute  $J_s$  fluxes

$$J_{total} = J_w + J_s \quad (58)$$

The solvent and solute fluxes are considered the same as those presented by Lonsdale et al. [25]. The pressure and osmotic pressure variances along the membrane are defined in Equations (59) and (60), respectively.

$$\Delta P = P_r - P_p \quad (59)$$

$$\Delta \pi = n_s R T (C_w - C_p) \quad (60)$$

The number of ions per salt molecule is represented as  $n_s$  (e.g.,  $n_s = 2$  for NaCl).

### 3.16. Model of Al-Obaidi et al.

Al-Obaidi et al. [43] developed a robust, steady-state model for the SW RO process to estimate the performance of multistage, multi-pass, medium-sized SW brackish water plant. The assumptions made are the same as those of Lonsdale et al. [25]. Further assumptions were made:

- The membrane is quantified as a porous flat sheet with a feed spacer.
- Constant membrane features and channel geometries.
- The relationship of Da Costa et al. [44] is used to estimate the pressure drop inside the feed side. This includes the pressure drop caused by the feed spacer.
- The fouling factor is included to mimic real operation of the RO process.

#### Model Equations

The authors proposed several new expressions for rejection and water recovery rate in addition to the practice of detailed relationships to evaluate the influence of feed temperature on model transport parameters. The influence of control variables on the fluid physical properties was considered with varying mass transfer coefficient and concentration polarisation. The total water flux  $J_w$  (m<sup>3</sup>/s) is expressed as

$$J_w = A_w NDP_{fb} A_m \times 10^5 \quad (61)$$

The net motivating pressure of feed and retentate is represented as  $NDP_{fb}$  (Pa), and  $A_w$  is the actual water transport parameter (m/s Pa) that has been estimated by relying on the reference value at 25 °C and temperature correction factor as

$$A_{w(T)} = A_{w(25\text{ C})} TCF_p F_f \quad (62)$$

The water permeability coefficient at (25 °C) is represented as  $A_{w(25\text{ C})}$  (m/s Pa), and  $TCF_p$ , and  $F_f$  are the temperature correction factor of permeate at standard conditions (dimensionless) and the fouling factor (dimensionless), respectively.

The solute flux via the membrane is expressed as

$$J_s = B_s (C_w - C_p) \quad (63)$$

The actual solute transport constant relying on the reference value at 25 °C is  $B_s$ , and is defined as

$$B_s = B_{s(25\text{ C})} TCF_s \quad (64)$$

The solute transport constant at 25 °C and the temperature correction factor of solute at ordinary conditions are expressed as  $B_{s(25\text{ C})}$  (m/s) and  $TCF_s$  (dimensionless), respectively.

Table 1 summarises the main characteristics and shortcomings of the selected literature models of SW membranes in RO processes. The table also shows the progress of process modelling in this area.

**Table 1.** Summary of the models developed for spiral wound reverse osmosis (RO) process.

Author and Year	Main Characteristics	Shortcomings
(Lonsdale et al., 1965)	<ul style="list-style-type: none"> <li>• A homogeneous diffusion model for cellulose acetate membrane.</li> <li>• Explained the transport phenomena through membrane films in the RO process.</li> <li>• Solvent and solute are dissolved in the nonporous surface layers of the membrane.</li> </ul>	<ul style="list-style-type: none"> <li>• Constant pressure throughout the membrane channels.</li> </ul>
(Avlonitis et al., 1991)	<ul style="list-style-type: none"> <li>• Considering the pressure loss occurred in brine and permeate channels.</li> <li>• Brine and permeate friction parameters, and membrane water permeability constant were integrated.</li> </ul>	<ul style="list-style-type: none"> <li>• The osmotic pressure and the concentration polarisation were ignored.</li> </ul>
(Boudinar et al., 1992)	<ul style="list-style-type: none"> <li>• Involved the main parameters affecting the performance of a spiral wound module.</li> </ul>	<ul style="list-style-type: none"> <li>• Constant fluid density.</li> <li>• Neglected the pressure drop along the permeate tube.</li> </ul>
(Avlonitis et al., 1993)	<ul style="list-style-type: none"> <li>• Considered the thin film theory to characterise concentration polarisation.</li> <li>• The concentration gradient along the membrane feed channel was embedded.</li> </ul>	<ul style="list-style-type: none"> <li>• Neglected the solute–solute interaction in multi-component solutions.</li> </ul>
(Abbas and Al-Bastaki, 2001)	<ul style="list-style-type: none"> <li>• Turbulent and laminar flow regimes were considered.</li> <li>• Represented a decay in water flux as a result of membrane fouling.</li> </ul>	<ul style="list-style-type: none"> <li>• Ignored the solute–solute interaction.</li> <li>• Eliminated the description of the membrane transport mechanism.</li> </ul>
(Marriott and Sørensen, 2003)	<ul style="list-style-type: none"> <li>• Described the flow patterns inside a SW module and characterised the main features of the membrane.</li> <li>• The pressure drop of flow was characterised by the friction parameter.</li> <li>• The stagnant film model presented the concentration polarisation.</li> </ul>	<ul style="list-style-type: none"> <li>• The permeate flow area was assumed constant.</li> </ul>
(Abbas and Al-Bastaki, 2005)	<ul style="list-style-type: none"> <li>• Investigated a neural network model (NNM) to guess the RO performance.</li> </ul>	<ul style="list-style-type: none"> <li>• The diffusivity, viscosity, and density were assumed constant.</li> </ul>
(Geraldés et al., 2005)	<ul style="list-style-type: none"> <li>• Improved a steady state distributed model for a SW RO process.</li> <li>• Mass and momentum transport inside the membrane modules were realised.</li> </ul>	<ul style="list-style-type: none"> <li>• Ignored the pressure change inside the permeate channels.</li> <li>• Ignored diffusion flow inside the feed side.</li> </ul>
(Avlonitis et al., 2007)	<ul style="list-style-type: none"> <li>• Two-dimensional flow equations were developed.</li> <li>• Easy to be used for any membrane with a bit modification for the water and solute permeability constants.</li> </ul>	<ul style="list-style-type: none"> <li>• Ignored the permeate concentration compared to the feed concentration.</li> </ul>

Table 1. Cont.

Author and Year	Main Characteristics	Shortcomings
(Majali et al., 2008)	<ul style="list-style-type: none"> <li>Developed semi-empirical and permeability models for two types of pilot scale RO plants.</li> </ul>	<ul style="list-style-type: none"> <li>Comprehensive mixing conditions were presumed in the feed and permeate channels.</li> <li>The semi-empirical model assumed fixed salt retention and water recovery.</li> <li>Fixed permeability coefficients for water and salt fluxes across the membrane are assumed.</li> </ul>
(Oh et al., 2009)	<ul style="list-style-type: none"> <li>A simple model relying on the solution–diffusion principles was developed that signifies the mechanisms of multiple fouling of an SW RO system.</li> </ul>	<ul style="list-style-type: none"> <li>The diffusion coefficient was unrelated to solute concentration.</li> <li>Fixed mass transfer parameter for a specified fluid condition.</li> </ul>
(Lee et al., 2010)	<ul style="list-style-type: none"> <li>A dynamic model was developed to explore the dynamic features and process operation of a large-scale RO desalination plant.</li> </ul>	<ul style="list-style-type: none"> <li>Dynamic fouling was not involved.</li> </ul>
(Kaghazchi et al., 2010)	<ul style="list-style-type: none"> <li>A steady state model was provided for an SW membrane module to examine the performance of two industrial seawater RO plants.</li> </ul>	<ul style="list-style-type: none"> <li>Ignored the effect of surface charge, pore length, tortuosity, bound water, and molecular shape.</li> </ul>
(Ruiz-Saavedra et al., 2015)	<ul style="list-style-type: none"> <li>A modest model for the SW membrane RO process was investigated, relying on the solution–diffusion model.</li> </ul>	<ul style="list-style-type: none"> <li>Ignored the solute–solute interaction.</li> </ul>
(Kotb et al., 2015)	<ul style="list-style-type: none"> <li>A simple model for RO system was developed to study the concentration polarisation.</li> </ul>	<ul style="list-style-type: none"> <li>Fouling propensity was not precisely involved.</li> </ul>
(Dimitriou et al., 2017)	<ul style="list-style-type: none"> <li>A dynamic model for an SW RO process was established under a non-constant operating condition of pressure and flow rate.</li> </ul>	<ul style="list-style-type: none"> <li>Plug flow was assumed in both feed and permeate sides.</li> </ul>
(Al-Obaidi et al., 2018)	<ul style="list-style-type: none"> <li>A mathematical model for the multistage multi-pass medium-sized SW brackish water RO process was presented.</li> <li>Highlighted the fouling factor.</li> </ul>	<ul style="list-style-type: none"> <li>Absence of a specific formula to signify the membrane retardation due to fouling for a long operation time.</li> </ul>

#### 4. Overview of Simulation of a Spiral Wound RO Module

To obtain higher efficiency and economical use of the RO seawater desalination process, two important parameters must be maximized: the product water quality and quantity. These parameters are adversely impacted by the operating conditions, membrane fouling, hydrolysis, and compaction in the RO unit. Raising the feed pressure is one of the probable solutions to maintain constant productivity. However, this would cause a progress in production cost as a result to a higher constraint of energy for filtration. Therefore, in order to operate a RO plant efficiently, it is crucial to assess the process performance against the control variables via simulation. In essence, the process parameters are mainly affected by the characteristics of raw water and the efficiency of the pre-treatment scheme [10]. This section highlights an overview of the many simulation studies that have been carried out and deployed to predict the performance of the RO desalination system.

Costa and Dickson [45] used their model, which is based on Kimura–Sourirajan fundamentals, to conduct a simulation to investigate the performance of an SW RO membrane element under different control variables for a single solute system and with a different number of RO membrane modules in series. They included the influence of operating pressure, feed flow rate, and the number of modules arranged in a series configuration. Their simulation results showed that the recovery rate increased with increasing pressure but dropped dramatically with increasing feed flow rate. The recovery rate increased by about 10 times at a pressure of 29.6 atm when increasing the number of modules from 1 to 10.

Boudinar et al. [26] improved the performance of a spiral wound module on the basis of physical transportation phenomena via simulation. A wide range of feed conditions including concentration, pressure, and flow rate of the brine and permeate streams were considered. Their results showed that the brine velocity, pressure, and water flux had a significant role in limiting the thickness of the mass transfer boundary layer at the membrane wall, which in turn improved the SW membrane performance.

Abbas [23] explored the performance of an industrial medium-scale brackish water SW RO desalination plant (40 m<sup>3</sup>/day), which was designed in three tapered stages using their semi-rigorous steady-state model. Specifically, the influence of feed flow rate and operating pressure were tested on the plant performance for different membrane module arrangements. The simulation results showed a deterioration of the product quality as a result of increasing pressure and feed flow rate. This was attributed to a decrease in the net transmembrane pressure difference caused by the high-frictional pressure drop. However, both solute rejection and water production were improved at low-to-moderate feed pressures and feed flow rates. The influence of feed spacer on the calculation of pressure drop was also evaluated. This is basically carried out by including the total drag force of the feed spacer to calculate the pressure drop along the membrane length using the relationship of Da Costa et al. [44].

Hyung and Kim [46] appraised the consequence of feed parameters including temperature and pH on boron rejection on the performance of a seawater RO process on the basis of their mechanistic predictive developed model. They confirmed that boron rejection could be improved due to increasing pH, decreasing temperature, and increasing pressure.

Pais and Ferreira [47] evaluated the performance of an SW membrane-based industrial desalination plant over a working time of 454 days on the basis of the solution–diffusion model. They demonstrated that water and solute permeability constants are important pointers in assessing the membrane performance. The simulation results showed a decrease in water permeability coefficient due to the absence of membrane cleaning during a given period. On the other hand, salt permeability had significantly enlarged during the summer season as a result to the temperature impact.

Oh et al. [22] analysed the effect of several parameters including water flux, temperature, and fouling mechanism on the efficiency of an RO system over a wide set of feed conditions. Additionally, the impact of feed water temperature on the boron concentration and energy consumption in permeate was explored. They showed that the recovery ratio increased with increasing feed pressure. However, the energy consumption decreased with decreasing water flux despite the improvement of solute rejection. Furthermore, raising the feed temperature would decrease the specific energy

and boron rejection due to increasing boron concentration in the permeate channel. An optimum permeate flux and recovery ratio for a specific condition of boron concentration in permeate and energy consumption were investigated.

Mane et al. [48] simulated boron removal in pilot and full-scale, single-stage, single-pass RO processes on the basis of six and eight SW membrane elements in a series to treat seawater. The model considered different water quality and operating conditions. Their results showed that boron rejection decreased due to a decrease in pressure and pH or an increase in temperature. Moreover, boron removal was found to be mainly influenced by the overall water recovery.

Kaghazchi et al. [20] simulated two industrial seawater RO desalination plants utilising SW membrane modules. A semi-rigorous mathematical model was used to examine their performance under various feed conditions of feed pressure and flow rate. Results exhibited that any growing of feed flow rate would cause a decrease in the permeate concentration due to increasing mass transfer coefficient and concentration polarisation. In addition, increasing the operating pressure increased the water flux with non-linear behavior, despite increasing the salt concentration along the feed channel that promoted the osmotic pressure.

Farhat et al. [49] investigated the performance of a new cohort of RO membranes of two-pass configuration to remove boron from seawater from the Arabian Gulf. Specifically, the impact of operational parameters of the second pass including feed water concentration, pressure, bulk velocity, and temperature on boron removal was assessed. Their simulation results showed that 96% of boron removal from brackish water can be achieved with low temperatures, high feed flow velocities, and high pressure. However, with high feed temperatures, boron removal decreased markedly.

Kotb et al. [50] studied the influence of feed characteristics and membrane module sizes on the salt concentration at the membrane surface using a simple model. They examined the effect of feed features (feed concentration and feed flow rate), control variables (feed temperature and feed pressure), and membrane dimensions on the salt concentration at the surface of each membrane. Results showed a decrease in the wall concentration as a result of increasing feed flow rate and feed temperature, while it increased with increasing feed pressure, feed concentration, and membrane area. As well as this, increasing the feed temperature was found to be more practicable in order to reduce the wall concentration when compared with decreasing the feed pressure and increasing the feed flow rate. This is attributed to the high energy consumption in the case of increasing pressure. More specifically, raising the temperature from 25 to 50 °C would reduce the membrane surface concentration by 23%. They concluded that the wall concentration was nearly double the feed concentration as a result of increasing the temperature from 25 to 35 °C. Consequently, the wall concentration was condensed by 7%, whereas the flow rate and pressure were increased by 2%.

Al-Obaidi et al. [43] simulated the operating conditions of TDS in a lower than 2 ppm multistage, multi-pass, medium-sized spiral wound brackish water RO desalination system belonging to the Arab Potash Company. Simulations were carried out to study the effect of increasing by 20% the operating conditions from the base case of actual plant data against numerous operating parameters including feed concentration, feed flow rate, feed pressure, and feed temperature. Results confirmed that both feed flow rate and pressure had a positive contribution on the product salinity.

Table 2 summarises the simulation results of the selected literature of the SW RO system.

**Table 2.** Summary of the previous work of RO simulation.

<b>Authors and Year</b>	<b>Highlighted Characteristics</b>	<b>Simulation Results</b>
<b>(Costa and Dickson, 1991)</b>	<ul style="list-style-type: none"> <li>• Predicted the performance of an SW RO membrane element on the basis of various feed conditions for a single solute system.</li> </ul>	<ul style="list-style-type: none"> <li>• Recovery rate increased with increasing pressure.</li> <li>• Recovery rate decreased with increasing flow rate.</li> </ul>
<b>(Boudinar et al., 1992)</b>	<ul style="list-style-type: none"> <li>• Investigated the performance of two types SW modules against the concentration, pressure, and flow rate of the brine and permeate streams.</li> </ul>	<ul style="list-style-type: none"> <li>• The thickness of the mass transfer boundary layer was affected by the brine velocity, flux, concentration, and pressure.</li> </ul>
<b>(Dickson et al., 1994)</b>	<ul style="list-style-type: none"> <li>• Predicted the performance of brackish water SW membrane module of RO system in terms of the module separation and recovery.</li> </ul>	<ul style="list-style-type: none"> <li>• A linear relationship between the feed concentration and osmotic pressure.</li> </ul>
<b>(Abbas and Al-Bastaki, 2005)</b>	<ul style="list-style-type: none"> <li>• Explored the performance of a SW membrane of a medium-scale brackish water RO desalination system on the basis of the feed flow rate, pressures, and the membrane module arrangement.</li> </ul>	<ul style="list-style-type: none"> <li>• High operating pressures led to a weakening in product quality.</li> <li>• High flow feed rates led to a drop in the water production and permeate quality.</li> </ul>
<b>(Hyung and Kim, 2006)</b>	<ul style="list-style-type: none"> <li>• Estimated the performance of full-scale SW RO processes on the basis of studying the influence of pH and temperature on boron removal.</li> </ul>	
<b>(Pais and Ferreira, 2007)</b>	<ul style="list-style-type: none"> <li>• Studied the performance of an SW membrane desalination system on the basis of water and solute permeability coefficient evolution.</li> </ul>	<ul style="list-style-type: none"> <li>• Water permeability coefficient was decreased due to the absence of membrane cleaning during the considered period.</li> <li>• Salt permeability enlarged during the summer due to temperature increases.</li> </ul>
<b>(Oh et al., 2009)</b>	<ul style="list-style-type: none"> <li>• Simulation study was achieved to predict the performance of a RO plant at any operating conditions.</li> </ul>	<ul style="list-style-type: none"> <li>• Recovery ratio increased with increasing feed pressure.</li> <li>• Specific energy consumption decreased with decreasing water flux.</li> <li>• Increasing the feed temperature would decrease the specific energy and boron rejection due to increasing the boron concentration in the permeate channel.</li> </ul>

Table 2. Cont.

Authors and Year	Highlighted Characteristics	Simulation Results
(Mane et al., 2009)	<ul style="list-style-type: none"> <li>Analysed the boron rejection of a pilot and full-scale for single-stage, single-pass RO processed on the basis of six and eight SW elements to treat seawater.</li> </ul>	<ul style="list-style-type: none"> <li>Boron rejection decreased due to a decrease in pressure and pH or an increase in temperature.</li> <li>Boron rejection was mainly affected by the overall process recovery.</li> </ul>
(Kaghazchi et al., 2010)	<ul style="list-style-type: none"> <li>Investigated the operation and performance of two industrial seawater RO plants on the basis of SW membrane modules.</li> </ul>	<ul style="list-style-type: none"> <li>At higher feed flow rate, concentration polarisation was neglected.</li> <li>Increasing feed flow rate caused a decrease in the permeate concentration.</li> <li>Increasing operating pressure increased the water flux with non-linear behaviour.</li> </ul>
(Farhat et al., 2013)	<ul style="list-style-type: none"> <li>Studied the performance of a new group of RO membranes under a two-pass arrangement and without any pH alteration to remove boron from seawater.</li> </ul>	<ul style="list-style-type: none"> <li>Lower boron removal was obtained with high feed temperatures.</li> <li>Boron elimination was influenced by feed concentration, membrane material, pH, bulk velocity, feed pressure, and temperature.</li> </ul>
(Kotb et al., 2015)	<ul style="list-style-type: none"> <li>A considerable range of control variables was investigated on the concentration polarisation of an SW module.</li> </ul>	<ul style="list-style-type: none"> <li>Increasing the module area, feed concentration, and feed pressure would increase the concentration at the membrane wall.</li> <li>Increasing feed temperature and flow rate would decrease the wall concentration.</li> </ul>
(Al-Obaidi et al., 2018)	<ul style="list-style-type: none"> <li>Simulated the performance of a low-salinity multistage multi-pass, medium-sized SW brackish water RO desalination plant.</li> </ul>	<ul style="list-style-type: none"> <li>The feed flow rate and feed pressure positively affected the permeate salinity.</li> </ul>

## 5. Overview of Optimisation a Spiral Wound RO Process

Optimisation of the RO process has been presented with less attention in the last few decades when compared to modelling and simulation studies. Following to the modern progress in advanced numerical approaches, optimisation methods can hold complex problems in the operation and/or design of different manufacturing processes [51]. Implementation of the operating variables' set and designed values at plant start-up time would not assure predictable productivity due to operational instabilities. Therefore, it is important to set an amended set of optimal points of the specified operating conditions compared to the employing of designed and real plant data [52].

The optimisation studies of Hatfield and Graves, van der Meer and van Dijk, and Geraldès et al. [34,53,54] focused on maximising the permeate production and specific productivity in order to reduce the operational cost by manipulating the water recovery, feed flow rate, and pressure. Moreover, the arrangement of RO modules has also contributed to attaining the objective function. Specifically, the optimum design of RO process would guarantee the best connection between the feed and product streams of different stages. Many studies have also been carried out to diminish specific energy consumption by refining membrane permeability, as well as on the basis of varying the recovery ratio, salinity, membrane configuration, existence of energy recovery device, feed pressure, flow rate and temperature [22,55–57]. Previous studies on optimisation of RO processes using SW membranes are now reviewed.

Hatfield and Graves [53] formulated a nonlinear programming problem for a mathematical model of a RO system on the basis of brackish water desalination to optimise the product flux and predict the optimal configuration of modules regarding to construction temperature. They affirmed that the cost of produced water can be condensed by reducing the size of RO systems.

Boudinar et al. [26] predicted the improvement in performance of spiral wound RO modules on the basis of optimising the geometrical parameters at given operating conditions. They developed a computer simulation program considering the physical phenomena inside the module and the module geometry. The geometrical optimisation of the ROGA (membrane type) module was maximised at a set of operating conditions, which included the permeate flow per unit volume and the driving force.

Van der Meer and van Dijk [54] used two mathematical models to simulate capillary and SW modules in order to optimise the module design parameters including the feed and permeate channel porosity, capillary diameter, and height. They also optimised the feed pressure and flow rate. A growth in the water production of 100% was realised by optimising the capillary module configuration and operation conditions compared to the SW module.

Nemeth [58] optimised the performance of ultra-low-pressure RO membranes of an advanced hybrid system of ultra-low and standard RO membranes. The optimisation methodology led to around 30% higher permeate productivity of ultra-low-pressure membranes compared to standard membranes. Additionally, the permeate indicators were meaningfully upgraded from the low-pressure systems.

Wilf and Schierach [56] improved the long-term performance of RO membranes in order to attain a high recovery and high flux operation that satisfies the reduction of water production cost via optimising the operating conditions. A successful reduction of around 10% in water cost was obtained.

Villafafila and Mujtaba [59] developed an optimisation framework, subjected to general constraints for the RO process to maximise the recovery ratio using different energy recovery devices. The optimisation problem of the highest recovery ratio was solved using an effectual successive quadratic programming (SQP)-based method that included the determination of optimal control variables (feed flow rate and pressure) and design factors (total number of tubes, and internal diameter). They included, in the optimisation problem, the choices of energy recovery with various devices, including an improved energy recovery device (ERD), turbines, and pressure exchangers. Results showed an improvement on fresh water recovery by connecting a number of RO membranes in a series. They affirmed that the inclusion of ERD would reduce the operating costs and the energy consumption by more than 50%.

Bouguecha et al. [15] optimised the operation of a desalination plant coupled with a source of solar energy that operated itself in an intermittent mode with the aim of minimising the energy consumption related to water production cost. Results showed the contribution of the solar energy system.

Wilf and Bartels [60] optimised the design of a large-scale seawater RO desalination plant and decreased the fresh water production cost. They proved that the use of specific RO configurations such as one-stage array configuration, two-pass, split partial permeate treatment, and elevated pH seawater are essential in order to increase boron removal capacity. However, this causes an increase in operating cost. In this regard, the fresh water production cost was reduced as a result of applying high-efficiency ERDs or high-permeability membranes. As well as this, the increase of water permeability coefficient and decrease in the salt passage would contribute to the reduction of water production cost.

Geraldes et al. [34] optimised a single-stage arrangement and the control variables of a medium-sized SW RO (1000 m<sup>3</sup>/day) with two-stage SW modules to obtain the optimum design of a minimum specific fresh water production cost (objective function). In this regard, the optimum design of a single stage with seven membrane modules in a series reduced the fresh water production cost by 13.5% when compared with a typical system design (single stage of four membrane modules). They also claimed that the specific fresh water production cost could be further condensed by utilising two stages in a series structure, with seven membrane modules per pressure vessel. Specifically, a two-stage seawater RO decreased the fresh water production cost by around 5.5% compared to a single stage configuration.

Guria et al. [61] achieved a multi-objective optimisation based on a genetic algorithm (GA) for brackish and seawater desalination using tubular and SW modules. The optimisation aimed to minimise the cost of desalination while maximising the permeate flow rate. Results showed that the membrane area was the most vital decision variable for SW modules, whilst the pressure was the important variable for tubular modules.

Gilau and Small [62] used the model developed to optimise the performance of a small-scale seawater RO process connected to a renewable energy system. The optimisation targeted two objective function of maximising the water productivity and minimising the specific energy consumption besides attaining a high boron removal. They looked at achieving the lowest specific energy consumption.

Vince et al. [63] optimised the brackish water RO process within an environmental and economical method on the basis of a flexible superstructure optimization, that is, taking into consideration the arrangement of membrane modules and the number of membranes in each module. Their simulation results showed that employing seven membranes for both first and second stages would have a water recovery rate of 82%. In this respect, the performances of the RO process configurations were appraised by updated cost models, including electricity consumption and total recovery rate.

Djebedjian et al. [64] developed a methodology to optimise the performance of an RO desalination system by the employment of the genetic algorithms (GA) technique. They concluded that an optimal pressure variance along the membrane aids to maximise the permeate flux and satisfy the permeate concentration limitation.

Zhu et al. [65] optimised the energy consumption of a simple seawater RO desalination process by constraining a fixed permeate flow in the presence of a fluctuating feed salinity. The analysis confirmed the possibility of predicting the optimal pressure operation to increase the energy savings of the proposed system. In other words, the total energy consumption can be decreased by deploying the same permeate flow due to pressure fluctuation despite the variation of feed concentration. In addition, the impact of ERD, membrane hydraulic permeability, brine disposal cost, and pressure drop are outlined for a one-stage system. More importantly, the possible highest water recovery is recommended, especially when the cost of disposed brine is high.

Oh et al. [22] applied a simple model to explore the optimum operating conditions of a RO process, including the water recovery, water flux, temperature, and fouling mechanism to predict the lowest energy consumption and at the same time enhancing the permeate quality. The feasibility of water recovery was explored via optimisation that reduced the energy consumption at the highest solute rejection. Moreover, the feed temperature was found to have a significant impact on the RO process performance.

The minimisation of specific energy consumption for three different RO modules (one stage, one stage with ERD, and two stages) was investigated by Li [55]. The models were formulated as non-linear optimisation problems. He introduced a set of dimensionless parameters that signified the coupling between membrane properties and operating variables. The optimal solution to specific energy consumption normalised by the seawater concentration was merely dependent on a dimensionless parameter, which was a function of the hydraulic permeability, membrane area, feed flowrate, and concentration.

Kotb et al. [50] minimised the total operational cost of general superstructures of single-stage, two-stage, and three-stage RO system via optimisation, considering various operating conditions. They specifically recommended the application of a single-stage configuration to achieve permeate flow rates below 6 m<sup>3</sup>/h whilst minimising fresh water production cost. For fresh water flow rates of up to 12 m<sup>3</sup>/h, they recommend two-stage configuration, whereas three-stage configuration was found to be useful for production of higher flow rates.

Table 3 summarises the characteristics of the discussed optimisation research of RO processes.

**Table 3.** Summary of the past work of RO optimisation.

Authors and Year	Objective Function	Control Variables	Constraints	Results
(Hatfield and Graves, 1970)	<ul style="list-style-type: none"> <li>• Maximised the product flux.</li> </ul>	<ul style="list-style-type: none"> <li>• Operating temperature.</li> </ul>	<ul style="list-style-type: none"> <li>• Maximum number of modules per pressure vessel.</li> </ul>	<ul style="list-style-type: none"> <li>• The cost of produced water is reduced as a result of reducing the size of RO systems.</li> <li>• Predicted the optimal arrangement of modules in a specific stage.</li> </ul>
(Boudinar et al., 1992)	<ul style="list-style-type: none"> <li>• Optimised the geometrical parameters of an SW RO process.</li> </ul>	<ul style="list-style-type: none"> <li>• Flow rates, pressures, and concentrations in the brine and permeate channels.</li> </ul>	<ul style="list-style-type: none"> <li>• Adopting a more realistic model that takes into account the spiral geometry.</li> </ul>	<ul style="list-style-type: none"> <li>• A set of operating conditions was maximised, including the permeate flow per unit volume and driving force.</li> </ul>
(van der Meer and van Dijk, 1997)	<ul style="list-style-type: none"> <li>• Maximising the permeate productivity per module and minimising the losses in high-concentration and permeate channels and hydraulic pressure (minimising energy consumption).</li> </ul>	<ul style="list-style-type: none"> <li>• The operating conditions of feed pressure, and feed flowrate.</li> </ul>	<ul style="list-style-type: none"> <li>• Water production per module.</li> <li>• Pressure losses in feed and permeate sides.</li> </ul>	<ul style="list-style-type: none"> <li>• Improved the performance of the SW, that is, specific productivity.</li> <li>• An additional increase in performance of 100% can be obtained by optimising the arrangement and control variables of a capillary module.</li> </ul>
(Nemeth, 1998)	<ul style="list-style-type: none"> <li>• Optimised the performance of ultra-low pressure RO membranes in a novel system design.</li> </ul>	<ul style="list-style-type: none"> <li>• Pressure boosting</li> <li>• Utilising permeates throttling at the first stage.</li> </ul>	<ul style="list-style-type: none"> <li>• The hydraulic behaviour of the full-scale membrane water treatment system.</li> </ul>	<ul style="list-style-type: none"> <li>• The obtained cost savings by the ultra-low-pressure membranes are noteworthy.</li> <li>• The cost savings principally originate from energy savings.</li> </ul>
(Wilf and Schierach, 2001)	<ul style="list-style-type: none"> <li>• Improved the long-term performance of RO seawater and the cost discount of systems using UF (Ultra Filtration) pre-treatment.</li> </ul>	<ul style="list-style-type: none"> <li>• Recovery rate.</li> <li>• Permeate flux.</li> </ul>	<ul style="list-style-type: none"> <li>• Deployment of high-water recovery and flux operation needs an improved quality of the feed seawater.</li> </ul>	<ul style="list-style-type: none"> <li>• The economics of the desalting process is improved by increasing the recovery rate and water flux in seawater systems.</li> <li>• The collective savings due to operating cost, lower investment, and capability to optimise system control variables as a result to better seawater quality would cause around 10% decrease in total water production cost.</li> </ul>
(Villafila and Mujtaba, 2003)	<ul style="list-style-type: none"> <li>• Optimised the recovery ratio.</li> </ul>	<ul style="list-style-type: none"> <li>• Feed flowrate and pressure.</li> <li>• Total number of tubes and internal diameter are the design parameters.</li> </ul>	<ul style="list-style-type: none"> <li>• Optimised control variables are dependent on the constraints presented.</li> <li>• The optimal values are highly sensitive to changes in water and energy prices, in addition to seawater salinity.</li> </ul>	<ul style="list-style-type: none"> <li>• The energy consumption is reduced by up to 50% by using a pressure exchanger device.</li> </ul>

Table 3. Cont.

Authors and Year	Objective Function	Control Variables	Constraints	Results
(Bouguecha et al., 2004)	<ul style="list-style-type: none"> <li>Assessed the performances of a desalination plant with the aim of optimising its operation in terms of energy accessibility.</li> </ul>	<ul style="list-style-type: none"> <li>A continuous operating mode was utilised by eliminating the impacts of source variations.</li> </ul>	<ul style="list-style-type: none"> <li>Represent the time limit of the autonomous operating pilot.</li> </ul>	<ul style="list-style-type: none"> <li>The participation of the storage dissipation unit by means of solar energy.</li> </ul>
(Wilf and Bartels, 2005)	<ul style="list-style-type: none"> <li>Optimised the design of large-scale seawater RO desalination systems to evaluate the decreasing of desalted water costs.</li> </ul>	<ul style="list-style-type: none"> <li>The arrangement and control variables of current large seawater desalination systems.</li> </ul>		<ul style="list-style-type: none"> <li>A notable reduction of fresh water costs were evaluated as a result of high-permeability, high-rejection membranes, and high-efficiency ERDs.</li> </ul>
(Geraldés et al., 2005)	<ul style="list-style-type: none"> <li>Minimise the cost of water production.</li> </ul>	<ul style="list-style-type: none"> <li>Number of membrane modules in pressure vessel.</li> <li>Feed pressure and velocity.</li> </ul>	<ul style="list-style-type: none"> <li>Maximum concentration polarisation.</li> <li>Maximum permeate salt concentration.</li> </ul>	<ul style="list-style-type: none"> <li>The water cost can be condensed to 66.7 eurocent/m<sup>3</sup> for a two-stage SW RO unit compared to 81.4 eurocent/m<sup>3</sup> compared to a single-stage and four membrane modules (FilmTecSW30HR-380) per pressure vessel.</li> </ul>
(Guria et al., 2005)	<ul style="list-style-type: none"> <li>Maximise the permeate, minimise the cost of desalination, and minimise the permeate concentration.</li> </ul>	<ul style="list-style-type: none"> <li>The pressure difference along the membrane, the active membrane area.</li> <li>The membrane types.</li> </ul>	<ul style="list-style-type: none"> <li>Maximum throughput.</li> <li>Maximum permissible permeability coefficients.</li> </ul>	<ul style="list-style-type: none"> <li>To attain a maximum throughput, the permeability factor of water must be at the highest level.</li> </ul>
(Gilau and Small, 2008)	<ul style="list-style-type: none"> <li>Optimise the performance of RO process for high boron elimination and minimum specific energy consumption.</li> </ul>	<ul style="list-style-type: none"> <li>Specific energy.</li> <li>Boron concentration.</li> </ul>		<ul style="list-style-type: none"> <li>Total energy consumption was lessened by 70% by using an energy recovery turbine, a booster pump, and a suitable membrane.</li> <li>Water cost was reduced by 41% by using ERD.</li> </ul>
(Vince et al., 2008)	<ul style="list-style-type: none"> <li>Optimised the brackish water reverse osmosis process within an economical and environmental approach based on the flexible superstructure.</li> </ul>	<ul style="list-style-type: none"> <li>The arrangement of the membrane module.</li> <li>The number of membranes in a module.</li> </ul>	<ul style="list-style-type: none"> <li>Number of membranes used in the module configuration.</li> </ul>	<ul style="list-style-type: none"> <li>Low total costs can be obtained at high-water flux; however, desalination environmental effects and electricity consumption are still high.</li> <li>Low water flux permitted the attainment of lower electricity consumption in cases of using a larger membrane area that causes higher costs.</li> </ul>
(Djebedjian et al., 2008)	<ul style="list-style-type: none"> <li>Optimise the performance of RO desalination plant by the genetic algorithms (GA) to maximise permeate volumetric flow rate and satisfy the permeate concentration.</li> </ul>	<ul style="list-style-type: none"> <li>The pressure variance across the membrane.</li> </ul>	<ul style="list-style-type: none"> <li>The permeate concentration.</li> </ul>	<ul style="list-style-type: none"> <li>Permeate concentration reduced with increasing in water flux and the membrane pressure difference.</li> </ul>

Table 3. Cont.

Authors and Year	Objective Function	Control Variables	Constraints	Results
(Zhu et al., 2009)	<ul style="list-style-type: none"> <li>• Optimise the energy consumption for a simple model of RO water desalination process by creating a fixed water flux in the occurrence of fluctuating in the feed concentration of seawater and brackish water.</li> </ul>	<ul style="list-style-type: none"> <li>• Feed pressure.</li> <li>• Feed concentration.</li> </ul>	<ul style="list-style-type: none"> <li>• Membrane hydraulic permeability.</li> </ul>	<ul style="list-style-type: none"> <li>• Specific energy consumption can be markedly condensed, providing the same water flux.               <ul style="list-style-type: none"> <li>• Higher water recovery can be obtained, particularly when the brine stream disposal cost is high.</li> </ul> </li> </ul>
(Oh et al., 2009)	<ul style="list-style-type: none"> <li>• Optimising the design of a simple model of RO process for low energy requirement.</li> </ul>	<ul style="list-style-type: none"> <li>• Recovery ratio.</li> <li>• Permeate flux.</li> <li>• Temperature.</li> <li>• Fouling mechanism.</li> </ul>		<ul style="list-style-type: none"> <li>• Higher flux increased the solute retention but increased the specific energy consumption.</li> <li>• Increased temperature would cut the specific energy but worsens the rejection.</li> </ul>
(Li, 2010)	<ul style="list-style-type: none"> <li>• Minimisation of specific energy consumption.</li> </ul>	<ul style="list-style-type: none"> <li>• Several fixed RO configurations.</li> <li>• Energy recovery efficiency.</li> <li>• Driving force.</li> </ul>	<ul style="list-style-type: none"> <li>• Minimum recovery is constant.</li> </ul>	<ul style="list-style-type: none"> <li>• Specific energy consumption was reduced with a much better water recovery by using ERD.</li> </ul>
(Kotb et al., 2016)	<ul style="list-style-type: none"> <li>• Minimisation of total cost of fresh water production for an RO system.</li> </ul>	<ul style="list-style-type: none"> <li>• Feed pressure.</li> <li>• Membrane area.</li> <li>• Feed flow rate.</li> </ul>		<ul style="list-style-type: none"> <li>• Single-stage layout can cause a minimum cost of fresh water production.</li> <li>• Two-stage layout was endorsed for the directed water production of less than 12 m<sup>3</sup>/h.</li> <li>• Three-stage layout was endorsed for higher water production rates.</li> </ul>

## 6. Suggestions and Principle Ideas to Improve RO Processes

The improvement of all RO processes is essential in order to increase their effectiveness and to make them more economical and environmentally friendly. This literature review of modelling, simulation, and optimisation of RO processes has shown that there is room for improvement due to several shortcomings. Therefore, the authors would suggest the following points to rectify this challenge in future research:

- There is progress in RO process modelling. However, relaxing strict and familiar assumptions would be beneficial in generating more accurate models.
- Most of the models developed for RO processes have limited application and appended membrane fouling and pore blocking. Realising these parameters would enhance the prediction of the process performance for prolonged operation time.
- Implementing different types of membranes in a specific RO plant is a possible option. This would entail a set of different water and solute permeability constants that would affect the energy consumption. This is an interesting piece of research, especially for high concentration seawater. Moreover, optimisation of the RO process would aid in selecting the appropriate type of membrane in each stage in order to ensure the lowest energy consumption.
- The RO process can be designed with multistage of different orders to reflect the quality of the created water and economic perspectives. Thus, there is much concern to optimise the RO design to fulfil a specific requirement in a way to reduce the fresh water cost. This is highly recommended, especially for the hybrid systems of different processes including the thermal process and RO process.
- Complex method of optimisation such as particle swarm methodology, genetic algorithm, and species conservative genetic algorithm are rarely applied for seawater and brackish water RO processes. In this regard, intensive efforts need to be carried out, especially for multi-objective optimisation, in order to allocate the best cost-effective design of a multistage RO process under optimal energy options and environmental impact.
- It is conceivable to implement an effective treatment method to limit the disposal of high-concentration brine from RO processes into water bodies. Recycle of brine streams, evaporation, and hybrid systems comprising an RO process and thermal desalination are not widely used.

## 7. Conclusions

This study was carried out to review existing models that have been developed for simulation and optimisation of RO processes from 1965 until the present date. This study showed the evolution of RO process modelling and confirmed a lower convergence after comparing its prediction against the experimental data. In this regard, several simulation studies were presented that assessed the influence of operating conditions on the process indicators. Moreover, many optimisation studies have accurately obtained the optimal operational variables and process arrangement to guarantee the attainment of the objective functions with respect to the feasible process constraints. This study proposed several options for process improvement that can be applied to strengthen the modelling, simulation, and optimisation of RO processes besides making them more cost-effective. From this, this research is an effective tool for upcoming developers and designers to comprehend and locate the scope and limitations of RO process-based seawater and brackish water desalination.

**Author Contributions:** Conceptualization, A.A.A. and M.A.A.-O.; methodology, I.M.M.; formal analysis, A.A.A.; resources, A.A.A.; writing—original draft preparation, A.A.A. and M.A.A.-O.; writing—review and editing, I.M.M. and R.P.; visualization, R.P.; supervision, I.M.M. All authors have read and agreed to the published version of the manuscript.

**Funding:** This research received no external funding.

**Conflicts of Interest:** The authors declare no conflict of interest.

## References

1. Kim, Y.M.; Kim, S.J.; Kim, Y.S.; Lee, S.; Kim, I.S.; Kim, J.H. Overview of systems engineering approaches for a large-scale seawater desalination plant with a reverse osmosis network. *Desalination* **2009**, *238*, 312–332. [CrossRef]
2. W.H. Organization, D.-W. 2018. Available online: <https://www.who.int/news-room/detail/12-07-2017-2-1-billion-people-lack-safe-drinking-water-at-home-more-than-twice-as-many-lack-safe-sanitation> (accessed on 16 April 2019).
3. Mancosu, N.; Snyder, R.L.; Kyriakakis, G.; Spano, D. Water scarcity and future challenges for food production. *Water* **2015**, *7*, 975–992. [CrossRef]
4. Alghoul, M.; Poovanaesvaran, P.; Sopian, K.; Sulaiman, M. Review of brackish water reverse osmosis (BWRO) system designs. *Renew. Sustain. Energy Rev.* **2009**, *13*, 2661–2667. [CrossRef]
5. Greenlee, L.F.; Lawler, D.F.; Freeman, B.D.; Marrot, B.; Moulin, P. Reverse osmosis desalination: Water sources, technology, and today's challenges. *Water Res.* **2009**, *43*, 2317–2348. [CrossRef] [PubMed]
6. Global Water Desalination Market 2018–2025 Current Trends, D., Consumption Analysis, Key Insights, Business Overview and Future Growth Opportunity. 2018. Available online: <https://www.reuters.com/brandfeatures/venture-capital/article?id=48863> (accessed on 27 April 2019).
7. Burgi, P.H.; Cabrera, E.; Arregui, F.; Leiden, A. Water challenges in the 21st century. In *Water Engineering and Management through Time-Learning from History*; CRC Press/Balkema: Boca Raton, FL, USA, 2010; pp. 303–334.
8. El-Manharawy, S.; Hafez, A. Water type and guidelines for RO system design. *Desalination* **2001**, *139*, 97–113. [CrossRef]
9. Mehdizadeh, H. Membrane desalination plants from an energy–exergy viewpoint. *Desalination* **2006**, *191*, 200–209. [CrossRef]
10. Abbas, A.; Al-Bastaki, N. Performance decline in brackish water Film Tec spiral wound RO membranes. *Desalination* **2001**, *136*, 281–286. [CrossRef]
11. Nooijen, W.; Wouters, J. Optimizing and planning of seawater desalination. *Desalination* **1992**, *89*, 1–19. [CrossRef]
12. Islam, M.; Sultana, A.; Saadat, A.; Shammi, M.; Uddin, M. Desalination technologies for developing countries: A review. *J. Sci. Res.* **2018**, *10*, 77–97. [CrossRef]
13. Mohsen, M.S.; Jaber, J.O. A photovoltaic-powered system for water desalination. *Desalination* **2001**, *138*, 129–136. [CrossRef]
14. Abdallah, S.; Abu-Hilal, M.; Mohsen, M. Performance of a photovoltaic powered reverse osmosis system under local climatic conditions. *Desalination* **2005**, *183*, 95–104. [CrossRef]
15. Bouguecha, S.; Hamrouni, B.; Dhahbia, M. Operating analysis of a direct energy coupled desalination family prototype. *Desalination* **2004**, *168*, 95–100. [CrossRef]
16. Senthilmurugan, S.; Ahluwalia, A.; Gupta, S.K. Modeling of a spiral-wound module and estimation of model parameters using numerical techniques. *Desalination* **2005**, *173*, 269–286. [CrossRef]
17. Bhattacharyya, D.; Williams, M.; Ray, R.; McCray, S. *Membrane Handbook*; Van Nostrand Reinhold: New York, NY, USA, 1992.
18. Zhu, A.; Rahardianto, A.; Christofides, P.D.; Cohen, Y. Reverse osmosis desalination with high permeability membranes—cost optimization and research needs. *Desalin. Water Treat.* **2010**, *15*, 256–266. [CrossRef]
19. Ahmad, G.; Schmid, J. Feasibility study of brackish water desalination in the Egyptian deserts and rural regions using PV systems. *Energy Convers. Manag.* **2002**, *43*, 2641–2649. [CrossRef]
20. Kaghazchi, T.; Mehri, M.; Ravanchi, M.T.; Kargari, A. A mathematical modeling of two industrial seawater desalination plants in the Persian Gulf region. *Desalination* **2010**, *252*, 135–142. [CrossRef]
21. Additive. Manufacturing. Conwed Releases Impressive New Global Sustainability Report. 2020. Available online: <https://3dprint.com/124443/conwed-sustainability-report/> (accessed on 7 August 2019).
22. Oh, H.-J.; Hwang, T.-M.; Lee, S. A simplified simulation model of RO systems for seawater desalination. *Desalination* **2009**, *238*, 128–139. [CrossRef]
23. Abbas, A. Simulation and analysis of an industrial water desalination plant. *Chem. Eng. Process. Process Intensif.* **2005**, *44*, 999–1004. [CrossRef]

24. Al-Obaidi, M.; Kara-Zaitri, C.; Mujtaba, I.M. Scope and limitations of the irreversible thermodynamics and the solution diffusion models for the separation of binary and multi-component systems in reverse osmosis process. *Comput. Chem. Eng.* **2017**, *100*, 48–79. [[CrossRef](#)]
25. Lonsdale, H.; Merten, U.; Riley, R. Transport properties of cellulose acetate osmotic membranes. *J. Appl. Polym. Sci.* **1965**, *9*, 1341–1362. [[CrossRef](#)]
26. Boudinar, M.B.; Hanbury, W.; Avlonitis, S. Numerical simulation and optimisation of spiral-wound modules. *Desalination* **1992**, *86*, 273–290. [[CrossRef](#)]
27. Avlonitis, S.; Hanbury, W.; Boudinar, M.B. Spiral wound modules performance. An analytical solution, part I. *Desalination* **1991**, *81*, 191–208. [[CrossRef](#)]
28. Avlonitis, S.; Hanbury, W.; Boudinar, M.B. Spiral wound modules performance an analytical solution: Part II. *Desalination* **1993**, *89*, 227–246. [[CrossRef](#)]
29. Avlonitis, S.; Pappas, M.; Moutesidis, K. A unified model for the detailed investigation of membrane modules and RO plants performance. *Desalination* **2007**, *203*, 218–228. [[CrossRef](#)]
30. Wilf, M.; Klinko, K. Performance of commercial seawater membranes. *Desalination* **1994**, *96*, 465–478. [[CrossRef](#)]
31. Marriott, J.; Sørensen, E. A general approach to modelling membrane modules. *Chem. Eng. Sci.* **2003**, *58*, 4975–4990. [[CrossRef](#)]
32. Abbas, A.; Al-Bastaki, N. Modeling of an RO water desalination unit using neural networks. *Chem. Eng. J.* **2005**, *114*, 139–143. [[CrossRef](#)]
33. Sourirajan, S. *Reverse Osmosis*; Logos Press Ltd.: London, UK, 1970.
34. Geraldes, V.; Pereira, N.E.; Norberta de Pinho, M. Simulation and optimization of medium-sized seawater reverse osmosis processes with spiral-wound modules. *Ind. Eng. Chem. Res.* **2005**, *44*, 1897–1905. [[CrossRef](#)]
35. Majali, F.; Ettouney, H.; Abdel-Jabbar, N.; Qiblawey, H. Design and operating characteristics of pilot scale reverse osmosis plants. *Desalination* **2008**, *222*, 441–450. [[CrossRef](#)]
36. Mason, E.; Lonsdale, H. Statistical-mechanical theory of membrane transport. *J. Membr. Sci.* **1990**, *51*, 1–81. [[CrossRef](#)]
37. Lee, C.-J.; Chen, Y.-S.; Wang, G.-B. A dynamic simulation model of reverse osmosis desalination systems. In Proceedings of the 5th International Symposium on Design, Operation and Control of Chemical Processes, PSE ASIA, Singapore, 25–28 July 2010.
38. Lee, S.; Lueptow, R.M. Rotating reverse osmosis: A dynamic model for flux and rejection. *J. Membr. Sci.* **2001**, *192*, 129–143. [[CrossRef](#)]
39. Ruiz-Saavedra, E.; Ruiz-García, A.; Ramos-Martín, A. A design method of the RO system in reverse osmosis brackish water desalination plants (calculations and simulations). *Desalin. Water Treat.* **2015**, *55*, 2562–2572. [[CrossRef](#)]
40. Kotb, H.; Amer, E.; Ibrahim, K. Effect of operating conditions on salt concentration at the wall of RO membrane. *Desalination* **2015**, *357*, 246–258. [[CrossRef](#)]
41. Maskan, F.; Wiley, D.E.; Johnston, L.P.; Clements, D.J. Optimal design of reverse osmosis module networks. *AIChE J.* **2000**, *46*, 946–954. [[CrossRef](#)]
42. Dimitriou, E.; Boutikos, P.; Mohamed, E.S.; Koziel, S.; Papadakis, G. Theoretical performance prediction of a reverse osmosis desalination membrane element under variable operating conditions. *Desalination* **2017**, *419*, 70–78. [[CrossRef](#)]
43. Al-Obaidi, M.A.; Alsarayreh, A.A.; Al-Hroub, A.M.; Alsadaie, S.; Mujtaba, I.M. Performance analysis of a medium-sized industrial reverse osmosis brackish water desalination plant. *Desalination* **2018**, *443*, 272–284. [[CrossRef](#)]
44. Da Costa, A.; Fane, A.; Wiley, D. Spacer characterization and pressure drop modelling in spacer-filled channels for ultrafiltration. *J. Membr. Sci.* **1994**, *87*, 79–98. [[CrossRef](#)]
45. Costa, M.L.; Dickson, J. Modelling of modules and systems in reverse osmosis. Part I: Theoretical system design model development. *Desalination* **1991**, *80*, 251–274. [[CrossRef](#)]
46. Hyung, H.; Kim, J.-H. A mechanistic study on boron rejection by sea water reverse osmosis membranes. *J. Membr. Sci.* **2006**, *286*, 269–278. [[CrossRef](#)]
47. Pais, J.A.G.; Ferreira, L.M.G. Performance study of an industrial RO plant for seawater desalination. *Desalination* **2007**, *208*, 269–276. [[CrossRef](#)]

48. Mane, P.P.; Park, P.-K.; Hyung, H.; Brown, J.C.; Kim, J.-H. Modeling boron rejection in pilot-and full-scale reverse osmosis desalination processes. *J. Membr. Sci.* **2009**, *338*, 119–127. [[CrossRef](#)]
49. Farhat, A.; Ahmad, F.; Hilal, N.; Arafat, H.A. Boron removal in new generation reverse osmosis (RO) membranes using two-pass RO without pH adjustment. *Desalination* **2013**, *310*, 50–59. [[CrossRef](#)]
50. Kotb, H.; Amer, E.H.; Ibrahim, K.A. On the optimization of RO (Reverse Osmosis) system arrangements and their operating conditions. *Energy* **2016**, *103*, 127–150. [[CrossRef](#)]
51. Edgar, T.F.; Himmelblau, D.M.; Lasdon, L.S. *Optimization of Chemical Processes*, 2nd ed.; McGraw-Hill: London, UK; Boston, MA, USA, 2001.
52. Tanvir, M.; Mujtaba, I. Optimisation of design and operation of MSF desalination process using MINLP technique in gPROMS. *Desalination* **2008**, *222*, 419–430. [[CrossRef](#)]
53. Hatfield, G.B.; Graves, G.W. Optimization of a reverse osmosis system using nonlinear programming. *Desalination* **1970**, *7*, 147–177. [[CrossRef](#)]
54. Van der Meer, W.; Van Dijk, J. Theoretical optimization of spiral-wound and capillary nanofiltration modules. *Desalination* **1997**, *113*, 129–146. [[CrossRef](#)]
55. Li, M. Minimization of energy in reverse osmosis water desalination using constrained nonlinear optimization. *Ind. Eng. Chem. Res.* **2010**, *49*, 1822–1831. [[CrossRef](#)]
56. Wilf, M.; Schierach, M.K. Improved performance and cost reduction of RO seawater systems using UF pretreatment. *Desalination* **2001**, *135*, 61–68. [[CrossRef](#)]
57. Zhu, A.; Christofides, P.D.; Cohen, Y. Energy Consumption Optimization of Reverse Osmosis Membrane Water Desalination Subject to Feed Salinity Fluctuation. *Ind. Eng. Chem. Res.* **2009**, *48*, 9581–9589. [[CrossRef](#)]
58. Nemeth, J.E. Innovative system designs to optimize performance of ultra-low pressure reverse osmosis membranes. *Desalination* **1998**, *118*, 63–71. [[CrossRef](#)]
59. Villafafila, A.; Mujtaba, I. Fresh water by reverse osmosis based desalination: Simulation and optimisation. *Desalination* **2003**, *155*, 1–13. [[CrossRef](#)]
60. Wilf, M.; Bartels, C. Optimization of seawater RO systems design. *Desalination* **2005**, *173*, 1–12. [[CrossRef](#)]
61. Guria, C.; Bhattacharya, P.K.; Gupta, S.K. Multi-objective optimization of reverse osmosis desalination units using different adaptations of the non-dominated sorting genetic algorithm (NSGA). *Comput. Chem. Eng.* **2005**, *29*, 1977–1995. [[CrossRef](#)]
62. Gilau, A.M.; Small, M.J. Designing cost-effective seawater reverse osmosis system under optimal energy options. *Renew. Energy* **2008**, *33*, 617–630. [[CrossRef](#)]
63. Vince, F.; Marechal, F.; Aoustin, E.; Bréant, P. Multi-objective optimization of RO desalination plants. *Desalination* **2008**, *222*, 96–118. [[CrossRef](#)]
64. Djebedjian, B.; Gad, H.; Khaled, I.; Rayan, M.A. Optimization of reverse osmosis desalination system using genetic algorithms technique. In Proceedings of the Twelfth International Water Technology Conference, IWTC12, Alexandria, Egypt, 27–30 March 2008.
65. Zhu, A.; Christofides, P.D.; Cohen, Y. Effect of thermodynamic restriction on energy cost optimization of RO membrane water desalination. *Ind. Eng. Chem. Res.* **2008**, *48*, 6010–6021. [[CrossRef](#)]

